Electronic Supplementary Material (ESI) for Journal of Materials Chemistry C.
This journal is © The Royal Society of Chemistry 2022

Supplementary information

Halide perovskite memristor with ultra-high-speed and robust flexibility for artificial neuron applications

Lingzhi Tang[a,b], Yang Huang[a], Chen Wang*[b,c], Zhenxuan Zhao*[d], Yiming Yang[a], Jiming Bian[e], Huaqiang Wu[d], Zengxing Zhang[b,c] and David Wei Zhang[b,c]

[a] School of Microelectronics, Dalian University of Technology, Dalian Liaoning 116024, China
[b] State Key Laboratory of ASIC and Systems, School of Microelectronics, Fudan University, Shanghai 200433, China
[c] National Integrated Circuit Innovation Center, Shanghai 201203, China
[d] Institute of Microelectronics, Tsinghua University, Beijing 100084, China
[e] Key Laboratory of Materials Modification by Laser, Ion and Electron Beams (Ministry of Education), School of Physics, Dalian University of Technology, Dalian Liaoning 116024, China
* Corresponding author email address: chen_w@fudan.edu.cn (Chen Wang), zhaozhenxuan@tsinghua.edu.cn (Zhenxuan Zhao)

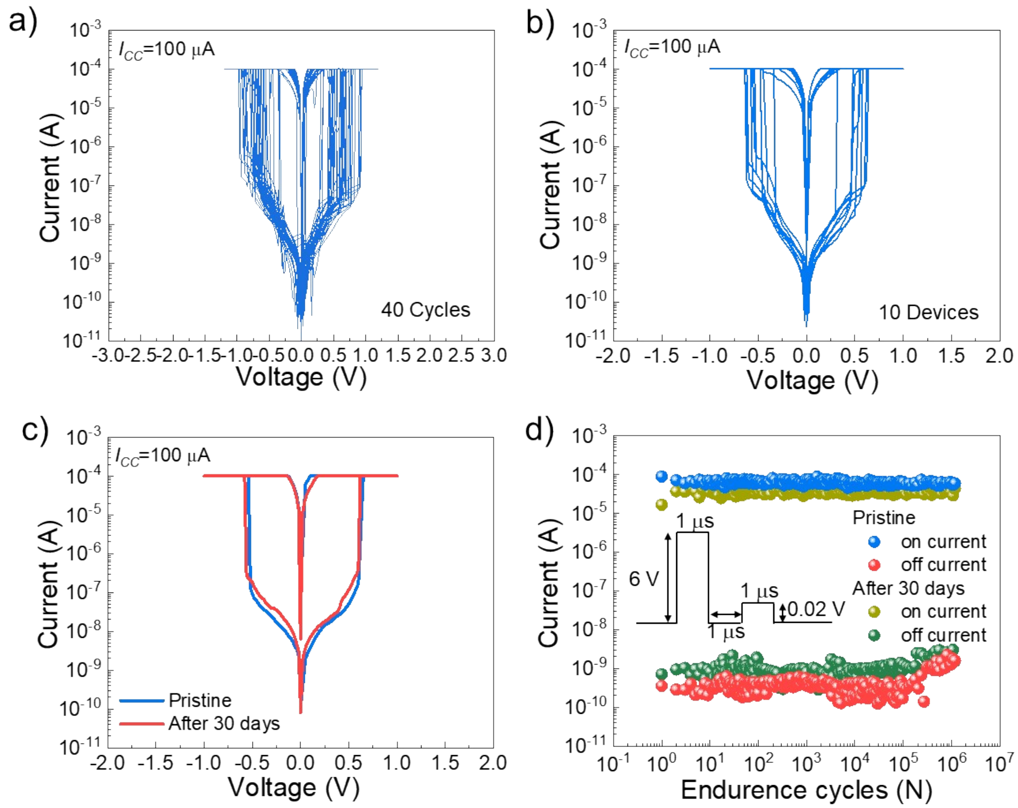

Fig S1. Results of operational and environment stability of devices. (a) 40 consecutive I−V curves of one TS memristor under an I_{CC} of 100 μA, (b) The DC *I-V* of ten randomly selected devices, (c) Long-term DC *I-V* characteristic under an I_{CC} of 100 μA after storage of 30 days, (d) Endurance characteristics after storage of 30 days. The inset shows the pulse voltages employed in the pulse measurement, which comprises a test voltage of 1 μs with an amplitude of 6 V and a read voltage of 1 μs with an amplitude of 0.02 V. All tests were done at room temperature (300 K) in dark, ambient conditions.

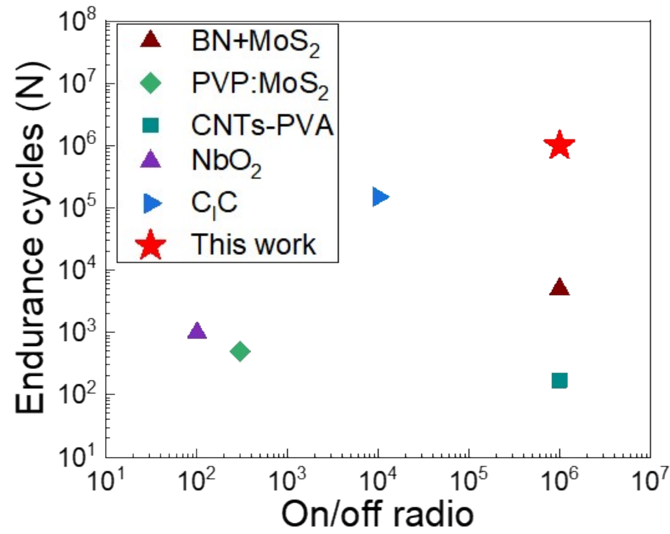

Fig S2. Comparison of endurance cycles and on/off ratios of various flexible TS memristors reported in representative works in recent years [1-5].

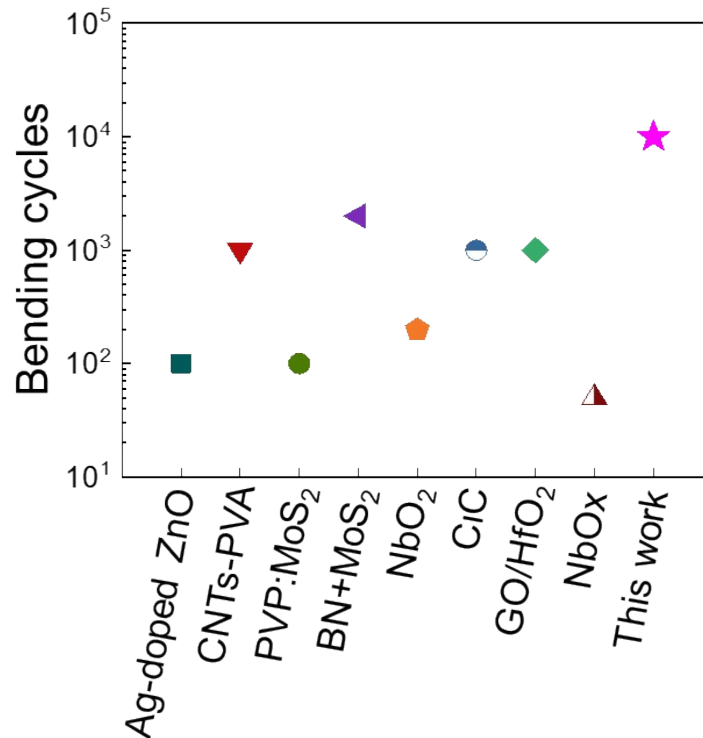

Fig S3. Comparison of bending cycles of flexible TS based on other materials in previous reports. Compared to other TS devices based on various dielectric materials, the flexible OIHP-based TS devices in this work can withstand more bending cycles

(10000 cycles) [1-8]. The flexible OIHP-based TS devices also showed stable in-situ DC *I-V* curves after maintaining convex bending for 180 h. However, other TS devices in Figure S3 have no research on in-situ electrical characteristics under the bending state.

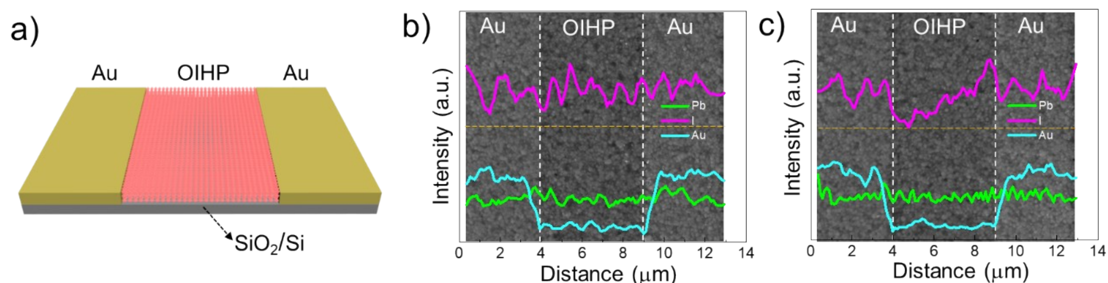

Fig S4. (a) The schematic diagram of Au/OIHP/Au planar structure. EDS line-scan profiles of I, Pb, Au elements along the yellow dotted line in (b)Before the voltage stimulation (c) After the voltage stimulation. It is challenging to characterize the filament corresponding to the threshold switching of devices because of its volatile characteristics. In this manuscript, we designed the Au/OIHP/Au planar devices fabricated using the same materials and preparation process as the vertical devices. The Au/OIHP/Au/ planar devices were prepared by the following steps. First, the Si substrates were cleaned in deionized water, acetone, and ethanol in order. Second, electrode patterns were generated by photolithography. Subsequently, the 10-nm-thick Ti layer and 40-nm-thick Au layer were deposited by e-beam evaporation. Finally, the Au electrodes were released by the lift-off process. Finally, the OIHP layer was spun using the same materials and preparation process as Ag/OIHP/Au/PEN vertical structure devices. The voltage stimulation applied on the right Au electrode was a

constant voltage of 3 V and the duration is 500-1000 s. The EDS was characterized immediately after voltage stimulation.

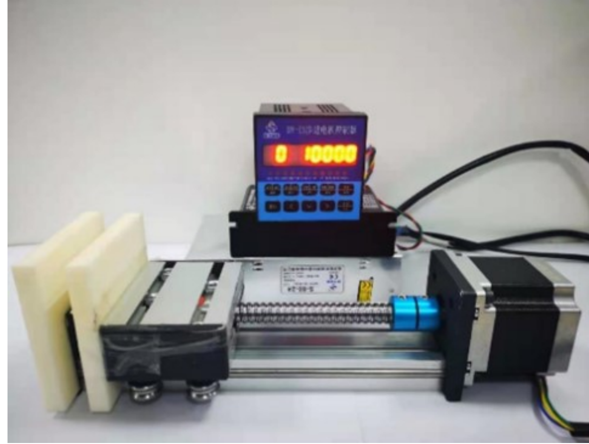

Fig S5. Custom-made mechanical bending machine used for flexibility measurement. The bending radius could be calculated by the formula $R=l/\theta$, where l is the width of the cell and θ is the corresponding circumference angle. The θ and bending radius can be configured by conditioning the forward step length. The bending process was carried out automatically until up to the set number.

Equations

The TRPL decay curves were fit by a biexponential decay function, as Equation (S1) shows[9]. The average carrier lifetime τ_{ave} was calculated by Equation (S2) [10]. The surface defect density N_t was calculated by Equations (S3-S4) [11]:

$$Y = A_1 \exp(-t/\tau_1)+A_2 \exp(-t/\tau_2)+ y0 \qquad \text{(S1)}$$

$$\tau_{ave} = A_1\tau_1 + A_2\tau_2 \qquad \text{(S2)}$$

$$1/\tau_{ave} = \alpha S/\sqrt{2} \quad \text{(S3)}$$

$$S = \sigma V_t N_t \quad \text{(S4)}$$

where τ_1 and τ_2 are the fast decay lifetime for nonradiative recombination and slow decay lifetime for radiative recombination, A_1 and A_2 are the relative amplitudes [9], τ_{ave} is the average lifetime [10], α is the absorption coefficient at the excitation wavelength ($\approx 10^5$ cm^{-1}) [12], S is the surface recombination rate (cm/s), σ is the typical recombination surface cross-section in semiconductors ($\approx 10^{-15}$ cm^{-2}), V_t is the carrier thermal velocity ($\approx 3.7*10^7$ cm/s), and N_t is the surface defect density per square centimeter [11].

Note

Figure 4(e)and (f) are low magnification SEM image of the surface of the OIHP film without any bending and after bending 10000 cycles for the same one sample. The characterization process is carried out in two phases. First, the OIHP film was characterized by SEM before bending. And then the same one sample was characterized again by SEM after bending 10000 cycles.

Reference

1. Y. Sun, D. Wen and F. Sun, *J. Alloys Compd.*, 2021, **869**, 159321.
2. Y. M. Sun and D. Z. Wen, *J. Alloys Compd.*, 2020, **844**, 156144.
3. I. Varun, A. K. Mahato, V. Raghuwanshi and S. P. Tiwari, *IEEE Trans. Electron Devices*, 2020, **67**, 3472-3477.
4. J. Ge, S. Zhang, Z. Y. Liu, Z. K. Xie and S. S. Pan, *Nanoscale*, 2019, **11**, 6591-6601.
5. K. J. Lee, Y. Chang, Chi , C. Lee, Jung , L. W. Wang and Y. H. Wang, *IEEE J. Electron. Devi*, 2018,

6, 518-524.

6. Y. Park, U. B. Han, M. K. Kim and J. S. Lee, *Adv. Electron. Mater.*, 2018, **4**, 1700521.
7. Y. Zhou, Z. T. Song, M. Zhu, H. Huang, J. Han, K. G. Chen, C. Ye, Z. Xu, S. H. Liang, W. Xiong and X. Chen, *IEEE J. Electron. Devi*, 2019, **7**, 1125-1128.
8. J. Zhu, Z. Wu, X. Zhang, Y. Wang, J. Lu, P. Chen, L. Cheng, T. Shi and Q. Liu, Chengdu, China, Apr，2021.
9. H. Lai, B. Kan, T. Liu, N. Zheng, Z. Xie, T. Zhou, X. Wan, X. Zhang, Y. Liu and Y. Chen, *J. Am. Chem. Soc.*, 2018, **140**, 11639-11646.
10. J. Xing, Y. Zou, C. Zhao, Z. Yu, Y. Shan, W. Kong, X. Zheng, X. Li, W. Yu and C. Guo, *Mater Today Phys*, 2020, **14**, 100240.
11. H. H. Fang, S. Adjokatse, H. Wei, J. Yang, G. R. Blake, J. Huang, J. Even and M. A. Loi, *Sci. Adv*, 2016, **2**, e1600534.
12. W. J. Yin, T. Shi and Y. Yan, *Adv. Mater.*, 2014, **26**, 4653-4658.